

Recent developments in the electrodeposition of nickel and some nickel-based alloys

RENÁTA ORIŇÁKOVÁ^{1,*}, ANDREA TUROŇOVÁ¹, DANIELA KLADEKOVÁ¹, MIRIAM GÁLOVÁ¹ and ROGER M. SMITH²

¹Faculty of Science, Institute of Chemistry, P.J. Šafárik University, Sk – 04101, Košice, Slovak Republic

²Department of Chemistry, Loughborough University, Loughborough, Leics, LE11 3TU, UK

(*author for correspondence, tel.: +421-55-6222605, fax: +421-55-6222124, e-mail: Renata.Orinakova@upjs.sk)

Received 11 May 2005; accepted in revised form 23 May 2006

Key words: alloys, electrodeposition, multilayers, nickel, powder material

Abstract

The numerous theoretical and practical studies of the electrodeposition of nickel and its binary and selected ternary alloys with copper and cobalt over the last 10–15 years are reviewed. The reported mechanisms of the electrodeposition processes and accompanying evolution of hydrogen are considered. The complex influence of different bath compositions, pHs, current densities or potential ranges and temperature on the formation of single or multiple deposition layers are compared. The determination of the structure and morphology of the deposits on different substrates, including solid surfaces and particulate materials, using a range of analytical techniques are reported.

1. Introduction

Although nickel electrodeposition has been studied since the beginning of the 20th century, there has been an increase in interest in recent years and it is now one of the most frequently used surface treatments. Electroplating is one of the few surface-finishing processes that can satisfy the requirements of decorative and functional applications. It promotes the appearance, extends the life, and improves the performance of materials and products in different media. Electrochemical methods of coating metallic layers are attractive due to the high degree of control obtainable by varying the experimental conditions. Metals, alloys, and composite layers can be deposited electrochemically to form single or multi-component layers. The recent interest in the electrodeposition of iron-group metals (Ni, Co, and Fe) and their alloys is due to their unique magnetic and thermophysical properties. For example, since the electrodeposition process is capable of depositing metals and alloys onto recessed and non-uniform surfaces, it has found a role in microelectromechanical systems (MEMS), which are the integration of mechanical elements, sensors, actuators, and electronics on a common silicon substrate through microfabrication technology [1].

In the present paper, we review studies of the electrodeposition of nickel and nickel based alloys over the last two decades, which have built on the extensive pioneering work of DiBari, Evans, Bockris, Matulis, Heusler, Weil, and Ives and many others [2–9]. The aim is to highlight new, and interesting, developments in nickel electrode-

position research and applications, and to indicate important trends in the field. The review gives an outline of the significant results, mechanisms and phenomena observed in the electrodeposition of nickel and of some of its alloys (especially Ni–Co and Ni–Cu). It also describes the different techniques applied in the electrodeposition process and in the investigation of electrodeposits.

2. Electrodeposition of nickel

Nickel and nickel alloys are used for a wide variety of applications, the majority of which require corrosion and heat resistance, including aircraft gas turbines, steam turbine power plants, medical applications, nuclear power systems, and the chemical and petrochemical industries.

Nickel deposition has been widely studied and much work has been devoted to the mechanism of the deposition process. The properties and structures of the electrodeposits are closely related to the electrolyte composition and electroplating parameters. For example, nickel sulphamate baths are widespread in high-speed electrodeposition, electroforming, and electrojoining processes because the resulting nickel deposits exhibit low internal stress and good ductility [10].

2.1. Mechanism of electrodeposition of nickel

A survey of the reaction mechanism, as well as the kinetics of nickel electrodeposition from different baths,

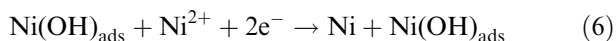
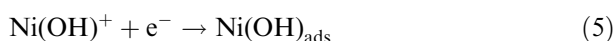
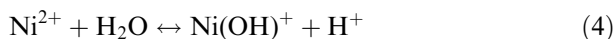
was given by Saraby-Reintjes and Fleischmann [11]. The generally accepted mechanism involves two consecutive one-electron charge transfers, and the participation of an anion with the formation of an adsorbed complex. This mechanism can be represented as:



The anion X^{-} has been variously assumed to be OH^{-} , SO_4^{2-} or Cl^{-} [11, 12]. By comparing the experimentally determined kinetic parameters with those calculated for the various rate-determining steps and ranges of coverage, they deduced that if a reaction mechanism of the general type (1)–(3) applied in a Watts bath (consisting of $\text{NiSO}_4 + \text{NaCl} + \text{H}_3\text{BO}_3$): (i) the anion X^{-} must be the chloride ion and (ii) the rate-determining step was reaction (2), i.e. the first-electron transfer step [11].

Allongue et al. [12], using *in situ* scanning tunnelling microscopy (STM) and cyclic voltammetry (CV), investigated the growth mechanism of ultrathin layers of nickel and cobalt that were electrodeposited from dilute sulphate solutions onto gold. The main difference between the two systems concerned the first adlayer, which is biatomic and strained by 4.4% in the case of cobalt, and is monoatomic and relaxed in the case of nickel.

Some studies of the electrochemical deposition of Ni have indicated that the nickel monohydroxide ion, NiOH^{+} , is an important species in the charge transfer steps in aqueous unbuffered solutions [13–16]:

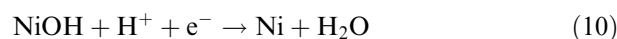
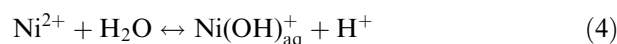


where $\text{Ni}(\text{OH})_{\text{ads}}$ represents the active intermediate, which may also be a chloride containing complex. Two one-electron metal reduction reactions take place in succession, giving rise to two clearly identifiable peaks in the cyclic voltammograms [16 and references cited therein]. Hydrogen evolution also occurred to different extents in the same potential region.

Cui and Lee [16] investigated nickel deposition from aqueous neutral chloride solutions in both the presence and the absence of oxygen. For voltammetric measurements, a rotating glassy carbon disc electrode or stainless steel electrode was used. Scanning electron microscopy (SEM) and stripping voltammetry were used for the analysis of the structure of the deposits and the determination of the current efficiency in deposition. In the presence of oxygen, the formation of a poorly

conductive layer of $\text{Ni}(\text{OH})_2$ on the electrode surface was observed, prior to nickel deposition because of oxygen reduction. This $\text{Ni}(\text{OH})_2$ layer inhibited the formation of a surface active nickel complex (formulated as $\text{Ni}(\text{OH})_{\text{ads}}^{+}$), and diminished both the nucleation and the growth of nickel. The effect was more pronounced in regions with little hydrogen evolution.

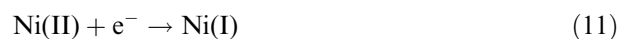
The electrolytic deposition of nickel from a Watts electrolyte solution onto a paraffin impregnated graphite electrode (PIGE) at pH 2, 3, and 4 was studied by Oriňáková et al. [17] and from the chloride electrolyte by Šupicová et al. [18]. Cyclic voltammetry and elimination voltammetry with a linear scan were applied. The latter provided a deeper insight into the mechanism of electrode reaction during metal deposition. The results indicated three steps in the deposition mechanism from the Watts electrolyte solution: (i) a chemical reaction preceding an electrochemical reaction, (ii) the occurrence of surface reactions with the adsorption of intermediates onto the PIGE and (iii) a reaction of the electroactive substance transported to the electrode by diffusion. Taking these results into account the reaction pathway of Bockris et al. [9] was assumed to be most relevant for nickel deposition:



The adsorption of chloride anions on the PIGE was detected from the chloride electrolyte. The elimination voltammetry indicated the importance of a kinetically controlled adsorption/desorption process in the nickel deposition mechanism (Equations (1)–(3)). Following the distribution diagram, the particle most likely to be electroactive at the start of electroreduction is NiCl^{+} [18].

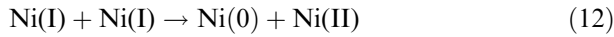
Similar results were obtained by Ji and Cooper [19]. They determined the nickel speciation in aqueous chloride solutions over a broad range of concentration and pH, and clarified the role of boric acid in nickel electrodeposition. They found that in concentrated NiCl_2 solution the predominant nickel species in the acidic region were Ni^{2+} and NiCl^{+} and in a concentrated mixed sulphate-containing NiCl_2 solution, Ni^{2+} , NiCl^{+} and NiSO_4 were important. The concentration of the NiOH^{+} species was negligible until the NiCl_2 concentration was lowered to $10^{-3} \text{ mol dm}^{-3}$.

The reduction of Ni(II) was one of the first steps in the mechanism proposed for nickel deposition by Gómez et al. [20]:

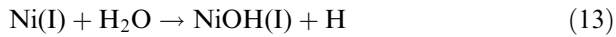


followed by either one or more steps that lead to the deposition. This simple scheme may apply at potentials

close to those just after start of the deposition (until the maximum potential of the reduction peak) and may explain the compact, uniform deposits obtained. At more negative potentials, the first step was maintained but was followed by a possible disproportionation reaction of Ni(I):



Moreover, under these conditions a simultaneous reaction may occur between Ni(I) and H₂O:

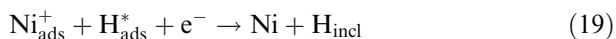
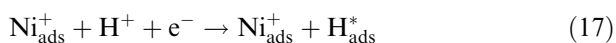


Reaction (13) explains the production of hydrogen during the nickel deposition.

Using voltammetric and potentiostatic methods, Gómez et al. [20] studied the initial stages of the deposition of nickel onto vitreous carbon from an aqueous chloride solution. The morphology of the deposit was observed by scanning electron and optical microscopy.

The mechanism of the Ni²⁺ reduction from acid sulphate, chloride and Watts electrolytes has also been extensively studied by Epelboin and Wiart and co-workers [21–26]. In an impedance study of nickel deposition, they observed that the electrode kinetics were dependent on the type of anion [23]. In chloride electrolytes, slow electrode activation with cathodic polarization was predominant. In sulphate solutions, the low-frequency capacitive feature, favoured by a pH decrease, appeared to result from interactions between the nickel and hydrogen discharges. An interpretation was proposed in which the ad-ion Ni_{ads}⁺ acts as both a reaction intermediate and a catalyst, associated with a propagating kink site, and where the adsorbed species H_{ads}^{*}, generated by the presence of Ni_{ads}⁺, inhibited the hydrogen evolution. It was concluded that the active area is closely connected to the extent of coverage by adsorbates.

Further impedance measurements showed that the electrolyte composition influenced the kinetics of nickel electrocrystallization [25]. The following mechanisms were suggested for electrolytes of pH 2–4 [25]:



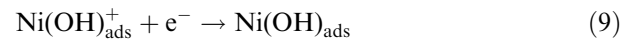
An electrochemical impedance spectroscopic (EIS) study of metal deposition by Wiart showed that the inhibition of the charge transfer was caused by adsorbates (hydrogen, anions, and additive molecules) or by

an interfacial layer [26]. EIS was also able to describe the growth of electrodeposits and gave access to the lifetime of active edges. Various examples (Cu, Ag, Ni, Zn) illustrated these situations.

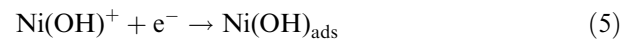
The electrodeposition from a low concentration of nickel onto vitreous carbon at pH 3 and 5 and with different anions has been studied by Proud and Müller [27] using EIS. They observed an adsorption process starting at potentials far removed from the potential corresponding to the deposition process. This process occurred more rapidly in chloride systems at pH 5 and more slowly in sulphate systems at pH 3 indicating that the adsorbing species was dependent primarily upon the pH of the system and secondly upon the anion. An overall mechanism was proposed based on the work of Wiart et al. [23, 25]. Reaction:



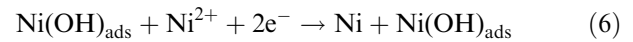
was the predominant step for the initiation of deposition at pH 5. The next step was:



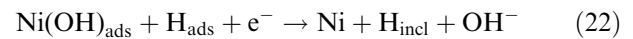
In the pH 3 system, the first step was the direct discharge of the hydroxylated complex:



Nickel deposition then took place *via* the steps:

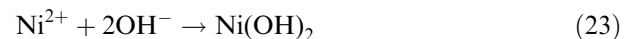


Protons were discharged simultaneously with nickel deposition:



The adsorbed hydrogen (H_{ads}) was responsible for the passivation observed at the lower potentials at pH 5. At higher potentials this intermediate tended to evolve gaseous hydrogen or produce hydrogen-containing forms of nickel (22).

The second passivation process occurred through the precipitation of a passivating coverage of the hydroxylated nickel species:



This passivation was eventually broken by the relative acceleration of other processes or the potential dependence of the reaction:



EIS was used by Holm and O'Keefe [28] to characterize the deposition of nickel onto stainless steel cathodes from unbuffered acid sulphate electrolytes at

pH from 2.0 to 3.5. The impedance spectra showed features, which were related to both the quality of the deposit and possible shifts in the deposition mechanism. The spectra for good quality nickel deposits consisted of a single, high frequency loop. As the deposit quality worsened, a second loop appeared at lower frequencies. The characteristics of this loop indicated the formation of a passivating nickel hydroxide layer, possibly resulting from the onset of diffusion control. The second loop was related to the presence of an oxidized nickel film which can form if the hydrogen ion concentration is low [28].

From the kinetic measurements during the electrodeposition of nickel, it was found that the rate of this discharge reaction was controlled by ion transport through the double layer. It had also been established experimentally that the rate-determining stage of the overall reaction was the single electron discharge of NiOH^+ to NiOH_{ads} [11, 21, 29, 30]. This offered the possibility of studying the time dependence of the current or potential during the transitional processes of nickel nucleation and growth.

Nickel nucleation onto glassy carbon substrates has been extensively studied. Bozhkov et al. [30] determined the concentration of nickel ad-atoms at the surface during the initial stages of nickel deposition onto glassy carbon substrates from the Watts electrolyte using both galvanostatic and potentiostatic pulse methods. They found that nickel ad-atoms carried a partial positive charge corresponding to about 25% of the total charge of the ion in the bulk of the solution.

2.2. Models of the electrodeposition process

Abyaneh and co-workers [31–33] proposed a model for the electrocrystallisation processes, following the application of a pre-pulse method. The transient equations derived on this basis were shown to closely fit the behaviour of the recorded pre-pulse transients for the electrocrystallisation of nickel onto a vitreous carbon electrode from Watts-type baths. The kinetic information about the initial nucleation and growth of the nickel deposit was obtained by analysing the experimental current–time transients. Nucleation rate constants were obtained over a range of deposition potentials.

The same group [34] studied the initial stages of the electrocrystallization of nickel and cobalt onto a vitreous carbon substrate by simultaneous ellipsometric and amperometric measurements during potentiostatic deposition. Nickel electrodeposition was carried out from a mixed sulphate–chloride electrolyte, and cobalt electrodeposition was carried out from a sulphate electrolyte. Theoretical equations adequately describing the optical transient data were derived.

Trevisan-Souteyrand et al. [35] also showed their stepwise computer model to be applicable to the potentiostatic current–time transient response of the nucleation of hemispherical centres and the radial

growth mechanism. Particular attention was devoted to the effects of the ohmic drop on the transient responses and on the number of growing centres. Computed values were compared to experimental transient curves and to transmission electron microscopy (TEM) micrographs obtained in the case of nickel electrocrystallization onto vitreous carbon.

Jensen et al. [36] investigated the process of nickel electrochemical deposition from Watts-type electrolytes under the influence of high frequency ultrasound. An improvement in the distribution of the deposited Ni in millimetre-sized groove-features on the cathode surface was observed.

Lemaire et al. [37] focused their work on nickel electrodeposition from an eutectic LiCl–KCl melt, which is the most frequently used molten salt in industrial processes. A discrete Fourier transform (DFT) analysis was carried out of the interfacial processes which occurred in the first steps of electrodeposition. By means of molecular modelling techniques, the most stable complexes were determined, and their interaction with the nickel cathode during electrodeposition process was studied. The results showed that complexes with more than four chlorine atoms were not stable.

The growth of the nickel film prepared by electrodeposition was described by Saitou et al. [38]. Two kinds of growth rate were measured using columnar photoresists formed on indium–tin oxide glass plates. The nickel film surface was analysed by atomic force microscopy. The ratio of the mean growth rate at the edge to that of the nickel layer indicated the presence of anisotropy between the up and down steps of the incorporation probabilities of the ad-atoms. Experimental results suggested that the nickel growth process had a dynamic scaling property.

A step-wise computer model for nickel electrodeposition from acidic solutions (pH 1) has been presented by Lantelme et al. [39]. The authors analysed the potentiostatic current–time transient response on glassy carbon or titanium with respect to nucleation and radial growth and developed a potentiostatic model for the electrodeposition of nickel at a rotating electrode. It was shown that the nickel deposition from acidic solutions onto glassy carbon or titanium obeys nucleation and hemispherical growth principles. A marked maximum in the current transients was observed for slightly acidic solutions (pH 4.5) and followed by a subsequent decrease in the deposition current. They attributed this behaviour to the early precipitation of nickel hydroxide due to a local increase in pH at the cathode surface. The results showed the influence of pH changes at the beginning of the deposition process.

2.3. Nucleation and growth of electrodeposits

The structural and magnetic properties of Ni films grown by electrodeposition from sulphate solutions onto GaAs surfaces have been studied by Evans et al. [40]. In-plane X-ray diffractometry was used to study the

nickel growth. The results showed that both the preferred growth relationship of growing film and the magnetic properties were strongly dependent on the substrate orientation.

According to Amblard et al. [41], the structure of the Ni electrodeposits grown on oriented substrates resulted in a competition between an epitaxial growth process and a non-epitaxial growth initiated by a substrate-independent nucleation. This independent nucleation was a necessary step prior to the progressive development of a definite fibre texture in thicker deposits. Both processes were investigated separately on two kinds of cathodic substrates: single crystals and amorphous carbon. For an amorphous substrate, multitwinned particles with a roughly hemispherical shape were generated by independent nucleation. Several competitive growth processes contributed to the whole current when the substrate was a low-index plane of a single crystal (Cu or Ni). Models were also proposed which accounted for the experimental current–time transients.

The same group discussed [42] the quantitative X-ray diffraction analysis of the fibre texture exhibited by the nickel electrodeposits obtained from a Watts bath. They investigated the preferred orientations exhibited by the Ni samples, which had been characterized by well-defined conditions of both preparation and X-ray diffraction analysis [43]. Experimental results described the quantitative modification of four different orientations – namely [110], [211], [100] and [210] – vs two relevant parameters, the pH of bulk solution and the minimum partial current density. The [100] orientation exhibited the character of a rather free growth, unlike the three other orientations. These were found to be associated with a definite chemical species (H_{ads} , $Ni(OH)_2$ or gaseous H_2) which selectively disturbed Ni electrocrystallization.

2.4. Additives to the electrolyte solution

Previous research showed that the addition of a modifier, such as boric acid, enhanced the electrowinning from high quality nickel deposits under a broad range of electrolyte parameters [28]. Inorganic additives showed little influence on the current efficiency. Increasing either the nickel concentration or the electrolyte temperature improved the current efficiency, while decreasing the pH significantly reduced the current efficiency [28]. The additives and operating parameters had a complex relationship in terms of their influence on the deposition mechanism.

Mockute and Bernotiene [44] examined the interaction of additives with the cathode during nickel electrodeposition in the Watts electrolyte. The interplay of saccharin, 2-butyne-1,4-diol and phthalimide, were studied by the determination of the consumption rates of the additives, of the accumulation rates of cathodic reaction products, and the incorporation of sulphur and carbon in the electrodeposits. A synergistic effect of the additives was observed. The aromatic compounds

increased additive adsorption by the carbonyl group, and 2-butyne-1,4-diol increased the adsorption of saccharin by the sulphonyl group.

In another study, the same authors [45] examined the reaction mechanism of some benzenesulphonamide and saccharin derivatives during nickel electrodeposition in the Watts electrolyte. It was found that the methyl group of *o*- and *p*-toluenesulphonamides and *N*-methylsaccharin increased the rates of the consumption of additives, mainly by the acceleration of desulphurisation reactions. The triple bond in the *N*-(2-butyne-4-ol) saccharin derivative complicated the reaction mechanism.

The effect of Cd^{2+} ions on the current efficiency, surface morphology and crystallographic orientation of the electrodeposited nickel from sulphate solutions has been studied by Mohanty et al. [46]. Their results indicated that Cd^{2+} ions did not have a significant effect on the current efficiency but caused a noticeable change in the surface morphology and deposit quality. X-ray diffractometry was used to study the crystallographic orientation of the electrodeposited nickel.

They also examined the effect of pyridine and its derivatives [47, 48] on the electrodeposition of nickel from aqueous sulphate solutions onto nickel and stainless steel substrates. The results indicated that the presence of additives did not have a significant effect on current efficiency, but changed the surface morphology of the deposits. The electrochemical reactions occurring during the deposition of nickel were examined by cyclic and linear sweep voltammetry techniques. Kinetic parameters, such as Tafel slope, transfer coefficient and exchange current density, were determined.

Froment and Wiart [24] also studied the effect of different organic inhibitors, especially 2-butyne-1,4-diol on nickel deposits from a Watts electrolyte on the basis of differential interferometry. The inhibiting action of an organic additive was characterised by a movement of the current density/cathode potential curve towards more negative potentials. The maximum amplitude was determined of the micro-relief of a deposit. Using impedance measurements, the process was also investigated in strongly acidic chloride and sulphate electrolytes and in electrolytes containing two additives: 2-butyne-1,4-diol and sodium benzenesulphonate [25]. The additives had a more pronounced inhibiting effect in chloride than in sulphate solutions. In chloride electrolytes, the inductive low-frequency effect was observed at more negative potentials than in additive-free electrolytes. With the addition of sodium benzenesulphonate in Watts or in chloride electrolytes, both an inductive and a capacitive low-frequency feature were present. These observations were interpreted on the basis of the specific effects of the anions. In sulphate electrolytes, the model involved the interaction between adsorbed hydrogen strongly bonded to the surface and the intermediate ad-ions Ni_{ads}^+ . In chloride electrolytes, the model was based on the slow desorption of an adsorbed anionic species.

Lin and co-workers [10] examined the influence of ammonium ions on the texture and structure of Ni deposits plated from a sulphamate bath onto a copper plate. The detailed microstructure of the Ni deposits was characterized using plane-view and cross-sectional TEM. The results indicated that the presence of ammonium ions in the bath created harder Ni deposits. The internal stress of the deposits also increased markedly when 100 ppm of ammonium ions was added.

2.5. Embedded particles

The fine dispersion of micro- or submicroparticles in a metal can lead to an improvement in the strength. The embedded particles can be selected to fulfil specific mechanical, electrical, piezoelectrical or magnetic properties in thin coatings. Ceramic particles, in particular, can lead to a tremendous increase in hardness in metallic materials [49, 50].

The electrodeposition of the Ni + SiC composite on unalloyed ductile iron has been investigated by Ibrahim et al. [50] using an acidic bath. The effect of the electrodeposition conditions on the incorporation of SiC into the deposit was studied. It was found that the volume percent of SiC particles in the composite layer increased with increasing current density and with the SiC concentration in the bath. The properties of the composite, such as hardness and wear resistance, were found to be significantly improved in comparison to the same properties of the uncoated substrate. It appeared economic to increase the wear resistance of a cast ductile iron by the application of the Ni + SiC composite by electrodeposition rather than by using heat treatment or the addition of expensive alloying elements.

The electrodeposition of Al₂O₃ particle-strengthened nickel films was carried out by Ferkel et al. [49] using galvanostatic deposition in a stirred Watts bath, with pH values from 2.5 to 4.5. The nickel films deposited on copper substrates were analysed by light and transmission electron microscopy and by energy dispersive X-ray (EDX) microanalysis. The embedded nanoparticles largely suppressed grain growth during heat treatment at higher temperatures. The particle-strengthened Ni films showed a remarkable improvement of hardness due to grain stabilisation and dispersion hardening of the nickel grains by the alumina nanoparticles.

Serek and Budniok [51] prepared composite Ni + Ti and Ni-P + Ti layers by simultaneous electrodeposition of nickel and titanium onto a steel substrate from a Watts bath under galvanostatic conditions. They examined the influence of the titanium powder content on the deposition process of the composite layers. The surface morphology of the coatings was examined by means of a stereoscopic microscope with a morphometric computer system. The phase composition was investigated by X-ray diffractometry. Atomic absorption spectroscopy was used for chemical characterization of the layers. It was found that an increase in the titanium powder in the bath resulted in an increase in the Ti embedded in the

composite layers. The presence of NaH₂PO₂ in the basic bath reduced the content of embedded Ti.

2.6. Substrate surface effects

The specific surface characteristics of the different substrates may modify the formation and morphology of the final deposit of nickel.

Gómez et al. [52] studied the influence of different metallic substrates on nickel electrodeposition from a chloride electrolyte. Cyclic voltammetry and potential step transient measurements were determined for platinum, nickel and iron electrodes. The surface of the electrodeposits was examined using a metallographic microscope and scanning electron microscopy and the microstructure was examined using transmission electron microscopy. Throughout the potential range, the total current resulted from two processes: nickel electrodeposition and hydrogen formation. For platinum electrodes, the hydrogen evolution was substantial. Simultaneous co-deposition of nickel and hydrogen favoured the nickel hydride structure, which was always formed at moderate negative limits. Atomic hydrogen was more easily adsorbed on electrodeposited nickel than on the nickel substrate. Nickel deposition was inhibited by the presence of H_{ads}, although the H_{ads} did not hinder the formation of a compact and coherent metallic deposit.

The same laboratory studied the micro-scale nickel electrodeposition on vitreous carbon in chloride medium [53, 54]. The nickel deposition was inhibited at some potentials and current densities, and was especially reduced at low concentrations and/or high pH values. This inhibition was related to two coupled reactions: a discharge of protons that produces an adsorbed species H_{ads} on deposited nickel, and hydroxide formation.

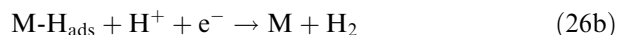
Correia et al. [55] used chronoamperometry to study the electrocrystallization of both Ni and Co onto vitreous carbon and gold substrates from dilute chloride baths. In addition, scanning electron microscopy and atomic force microscopy were used to visualise the morphology of the surface, in particular the overlap of growth centres. It was found that electrocrystallization was under diffusion control, and followed the Sharifker and Hills model.

The electrodepositions of Ni, Co and five Ni-Co alloys onto vitreous carbon electrodes from dilute chloride baths (pH 4.1–5.0) were studied by linear sweep voltammetry [56]. SEM studies of the different alloys revealed surface morphologies varying from a pure Ni nodular pattern to a fibrillar one, which are related to Co deposits. A regular deposition mechanism was proposed, contrary to the anomalous behaviour frequently observed. The regular deposition behaviour, confirmed by EDX analysis of the coatings, was associated with very thin deposits, which were not sufficient to promote anomalous behaviour. Dot mapping demonstrated a homogeneous distribution of Ni and Co atoms throughout the surface.

These authors [57] also studied the hydrogen evolution reaction on two different surfaces obtained by the electrodeposition of Ni and Hg onto Pt ultramicroelectrodes.

2.7. Hydrogen evolution

Hydrogen evolution reaction often occurs during Ni deposition in aqueous solution. There are two generally accepted mechanisms for this reaction [58 and references cited therein]: (i) discharge (Volmer reaction) (25) followed by Tafel recombination (26a) or (ii) discharge (25) followed by electrochemical desorption (Heyrovsky reaction) (26b):



The rate-determining step is determined by the strength of the hydrogen bond with the surface [12]. Reaction (25) is an adsorption step in which a chemical bond $M-H_{\text{ads}}$ is formed ($M = \text{Co}$ or Ni). A major portion of the adsorbed hydrogen reacts to give hydrogen molecules following a desorption stage according either to reaction (26a), which implies that H_{ads} are mobile on the surface, or to reaction (26b) in which a second proton is involved. A small proportion of the adsorbed hydrogen is adsorbed into the metallic lattice, $M(H_{\text{ads}})$ [58 and references cited therein] as follows:



It was assumed, that the adsorbed Ni species catalyse H-adsorption [12 and references cited therein] and the proportion of hydrogenated forms of electrodeposited nickel, α -nickel with low hydrogen content, and β -nickel richer in hydrogen, varied with the experimental conditions [29]. The α -nickel is a solid solution of hydrogen in nickel with an atomic ratio of (H/Ni) 0.03 whereas interstitial hydrogen atoms form β -nickel.

Most studies of the hydrogen evolution have been based on studies of the hydrogen overpotential in aqueous solutions. Bockris and Potter [59] measured the overpotential at nickel cathodes in aqueous solutions of HCl or NaOH. The course of the Tafel slope for nickel cathodes was investigated at several temperatures and concentrations. The most probable mechanism of hydrogen overpotential at nickel was a rate-determining discharge step followed by the recombination of hydrogen atoms. The discharge probably took place from hydroxonium ions in acid solution. The desorption step occurred relatively rapidly at the nickel cathode as a consequence of a low heat of desorption at high surface coverage.

The effect of the hydrogen reduction reaction on the initial stage of nickel electrodeposition from an acidic sulphate solution (pH 5.2) with or without the addition of boric acid was studied by Song et al. [58] using an electrochemical quartz crystal microbalance. Nickel was deposited onto the Pt-coated quartz crystal electrode under potentiodynamic conditions. In the absence of boric acid, the formation of nickel hydroxide at the electrode with simultaneous underpotential deposition of nickel was confirmed. Moreover, it was found that co-deposition of nickel and hydrogen occurred during the initial nickel deposition in a sulphate electrolyte with boric acid.

3. Electrodeposition of some Ni-based alloys

Nickel alloys with other metals and materials have made a significant contribution to our present-day society and promise to continue to provide materials for an even more demanding future. Our attention in this section is paid chiefly to Ni-Co and Ni-Cu alloys. Some interesting ternary alloys are also considered.

The alloys of the iron group metals often have a high hardness, high internal tension, and valuable magnetic properties. These materials are important for various practical reasons. The hardness and strength of the electrolytic deposited coatings is better than alloys prepared by conventional metallurgical procedures. In addition changes in the composition gives coatings which can stay light and brittle. They have a protective function and are resistant against wear and corrosion. They can be used for decorative purposes because their layer, in most cases, is of metal brightness, and some of them are coloured, which is also important.

Currently, more than 200 binary alloys are used in industry. The magnetic compounds are very interesting for various applications in computer technology and microelectronics, in the aircraft industry, and for coating plastics. The electrolytic deposition of these materials is a complex process and must be continuously controlled and regulated. The binary coatings are usually prepared from aqueous solutions or from melting salt electrolytes. Some practical aspects of the electrodeposition of iron group metal alloys were discussed by Liebscher [60]. Analysis of the electrodeposition of alloys using the distribution ratios of the two components was shown to be an effective tool either to control the composition of the deposit or to interpret the interaction between the components.

3.1. Electrodeposition of Ni-Co

Although Ni-Co films are widely used in protective and decorative plating applications, they are also used as permanent magnetic memories with a high commutation speed. As nickel-cobalt forms a solid solution over the whole concentration range [61], the ability of nickel and cobalt to alloy in all ratios enables the

potential uses of their magnetic properties to be explored in a wide range of conditions. In recent years, an increasing interest in the electrochemical deposition of alloys has emerged, mostly in the microelectronics industry, who use electrodeposition for microfabrication purposes, and in the surface treatment industry, which is confronted with the need for the development of new types of functional coating that are environmentally safe. Magnetic recording tapes, rocket technology and cosmonautics, composite coatings, and devices for photothermal conversion of solar energy are a few examples of the non-decorative uses of Ni–Co electrodeposition.

3.1.1. Mechanism of co-deposition

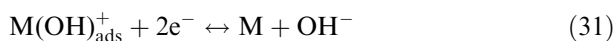
The electrodeposition of Ni–Co, whether from simple or complex baths, occurs in an anomalous manner [61]. The term anomalous co-deposition as introduced by Brenner [62] refers to the preferential deposition of the less noble metal rather than the more noble metal [56, 61, 63]. This phenomenon has been reviewed extensively for the iron group binary alloys and numerous models have been developed to predict this behaviour [15, 64–67]. However, although many models have been proposed, the mechanism of the anomalous co-deposition is not fully understood [68, 69]. One explanation for anomalous co-deposition is the formation of a hydroxide precipitate of the less noble metal at the cathode, caused by a local increase of pH. The hydroxide may suppress deposition of the noble metal [70]. However, recent studies showed that anomalous co-deposition occurred at a much lower pH at the electrode surface than that required for the formation of the metal hydroxide [15, 67, 70]. The generally accepted mechanism proposed for this electroplating behaviour, based on the formation and adsorption of the metal hydroxyl ions on the deposits, can be expressed as follows [71 and references cited therein]:



(side reaction on the cathode)



(electrostatic force of the cathode)



where M represents Co and Ni atoms. The newly formed OH^- in Equation (31) favours the further formation of MOH^+ and enhances the adsorption of MOH^+ . The adsorption ability of CoOH^+ is considered to be higher than that of NiOH^+ [71 and references cited therein].

An attempt to establish the cause of the anomalous co-deposition of nickel–cobalt alloys onto vitreous carbon electrodes from an acid chloride bath containing

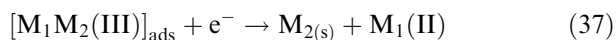
various ratios of metallic cations was made by Gómez et al. [61]. The electrochemical experiments were carried out under potentiostatic or potentiodynamic conditions. The morphology of the deposits was examined by SEM and varied with both bath composition and deposition potential. The results suggested the following sequence of events: nickel is always deposited first; then cobalt(II) adsorbs onto the freshly deposited nickel and begins to be deposited. The cobalt(II) adsorption inhibits subsequent deposition of nickel, although it does not block it completely. Simultaneously, cobalt deposition is catalysed since it is enhanced on the freshly deposited nickel compared to deposition on cobalt.

Anomalous nickel–cobalt electrodeposition onto a copper wire from a simple chloride bath and a complex ion bath were studied by Fan and Piron [70] at different current densities. The kinetics of the co-depositions were compared with those of individual nickel and cobalt depositions. It was found that the anomalous co-deposition only occurred with a simple chloride bath and could be related to the intrinsically fast kinetics of cobalt deposition.

Zech et al. [72] studied the co-deposition behaviour of three iron-group alloy systems (Ni–Co, Fe–Ni, Fe–Co) in acid sulphate electrolytes (pH 3) using copper rotating cylinder electrodes. An X-ray fluorescence (XRF) spectrometer was used to determine the composition and the thickness of the deposits. The result confirmed that co-deposition of the iron group metals led to a decrease in the reduction rate of the nobler component and an increase in the reduction rate of the less noble component compared to single metal deposition. A mathematical model for the anomalous co-deposition described the effects of the inhibition and enhancement observed experimentally [64, 73]. New experimental data on the iron–nickel alloy were presented, which suggested not only that iron inhibited the partial reaction of nickel but also that the addition of nickel may catalyse the deposition of iron. A model for a charge-transfer coupled co-deposition was proposed [73]. This was a generalization of the catalytic model for “induced” co-deposition by including the inhibition effects due to the adsorption of reaction intermediates, typically found in “anomalous” co-deposition. It was assumed that the deposition of each individual component M_j ($j = 1, 2$) followed a two-step reaction:



Parallel to the reaction sequence (32)–(35), reduction of the divalent species $\text{M}_j(\text{II})$ occurred by a catalytic reaction involving a mixed reaction intermediate, schematically represented by the formula $[\text{M}_1\text{M}_2(\text{III})]_{\text{ads}}$:



A set of rate equations was also proposed.

The inhibition of the anomalous co-deposition of the iron-group alloys (Co–Ni, Fe–Co, Fe–Ni, Zn–Fe, and Zn–Ni) on copper plates from chloride baths was studied by Bai and Hu using cyclic voltammetry and impedance spectroscopy [68, 71]. The average composition of the deposits was measured using EDX spectroscopy. It was found that the dissolution of the freshly deposited alloys and the co-dissolution of the adsorbed monohydroxide (MOH^+) layer in the anodic dissolution region depressed the propagation of more active metals and inhibited the anomalous co-deposition of the iron-group alloys. The effects of the electroplating variables (pH, temperature, potential range, and cycle number) on the composition and morphology of nickel–cobalt deposits plated by means of cyclic voltammetry were also investigated [71]. The Ni–Co deposits were electroplated onto copper plates from chloride baths at pH 2.0 and 3.0. The average composition of deposits was measured using EDX spectroscopy. The morphologies of the Ni–Co deposits were strongly dependent on the composition, the potential range of CV and the pH of plating baths. The grain size of Ni–Co deposits increased on increasing the number of cycles of CV deposition or the plating temperature.

In contrast to the anomalous type of deposition, Correia and Machado [56] using linear sweep voltammetry found a regular deposition behaviour for Ni–Co coated onto vitreous carbon electrodes from diluted chloride baths. Quantitative chemical analysis of the alloys showed a direct relationship between the bath and coating composition. The regular behaviour was associated with the very thin layers of deposit, which were not sufficient to promote anomalous behaviour. SEM studies of the different alloys revealed surface morphology varying from the pure Ni nodular pattern to a fibrillar morphology related to Co deposits.

The electrochemical behaviour of Ni–Co amorphous alloys G15 ($\text{Ni}_{58}\text{Co}_{20}\text{B}_{12}\text{Si}_{10}$) and G16 ($\text{Ni}_{25}\text{Co}_{50}\text{B}_{10}\text{Si}_{15}$) in carbonate–bicarbonate buffers of pH 8.9 to 10.5 were studied by Barbosa et al. [74] using voltammetry and stationary polarization techniques combined with electrochemical impedance spectroscopy and X-ray photoelectron spectroscopy (XPS). The results indicated that the electrochemical processes were dependent on the applied potential, the alloy composition, the pH value, and ionic strength of the electrolyte. Enhancement of the corrosion processes was observed when the pH and ionic strength were increased and when the Co content of the alloy was diminished.

3.1.2. Influence of the electrolyte composition

The co-deposition of nickel and cobalt can be carried out from different electrolytes: sulphate, chloride,

chloride–sulphate, or sulphamate solutions, either with or without additives. Among the additives, saccharin and sodium lauryl sulphate, as surfactants, boric acid and ammonium sulphate, principally as buffers, are very important [75]. The effects of current density, temperature and electrolyte pH on the energy consumption and the quality of nickel–cobalt deposits were studied by Lupi and Pilone [75] under galvanostatic conditions in acid sulphate medium. The surfaces of the cathodic deposits were examined and analysed by SEM–energy dispersive spectrometry (SEM-EDS). It was possible to obtain the both energy saving and a dense deposit without internal stresses, by optimisation of the operating conditions without the addition of surfactants.

The effect of the electrolyte composition and operating conditions on the Ni–Co composition, and the mechanism of its electrodeposition from a sulphamate electrolyte was studied by Golodnitsky et al. [76]. By chronoamperometric methods, they demonstrated that the rate-determining step of alloy deposition was the electrochemical reaction, complicated by the adsorption. The effects of different anionic additives (boric acid, sodium acetate, citric acid, glycolic acid, and oxalic acid) on the cathode reactions were studied [69]. Electrodeposition experiments were performed in a three-electrode system with a platinum rotating disk working electrode. X-ray fluorescence spectrophotometry was used for the compositional analysis of the electrodeposited alloys. The operating conditions under which the pH rise was inhibited were found. It was suggested that protonated citrate complexes are involved in alloy deposition. The acetate complexes do not participate directly in the cathode reaction. The results showed that Ni–Co electrochemical alloying leads to an increase in the reaction rate of cobalt at the expense of the nickel. The authors believed that the anomalous co-deposition of the Ni–Co alloy could be explained, along with pH change, competitive adsorption, and under-potential deposition, in terms of the crystal-field theory by the preferential reduction of high-spin cobalt(II) complexes.

Ni–Co alloys deposited from a sulphamate electrolyte with acetate and citrate-anion additives were evaluated for their structure and properties, such as microhardness, tensile strength, internal stress, and high-temperature oxidation [77]. Ni–Co alloys deposited from an electrolyte at pH 5, and at a current density higher than 5 A dm^{-2} included metal hydroxides, causing the formation of a more strained structure. Citrate complexes of Ni and Co eliminated the incorporation of hydroxides into the deposits and enabled a low-internal-stress coating to be formed.

Burzyńska and Rudnik [78] studied the effect of saccharin and sodium lauryl sulphate addition on the deposition of Ni–Co alloys onto stainless steel or titanium electrodes using a chloride–sulphate (Watts-type) electrolyte. The deposition of the Ni–Co alloys was conducted under galvanostatic conditions and the phase identification of the deposits was performed by X-ray diffraction analysis. It was found that the compo-

sition of the Ni–Co alloys may be controlled through the selection of the following parameters: cathodic current density, concentration of cobalt ions, and the addition of saccharin or sodium lauryl sulphate. The presence of these surfactants enabled the deposition of an alloy with a current efficiency of 99.7% and current densities up to 2 A dm^{-2} .

Goldbach et al. [79] investigated the electrochemical deposition of Ni–Co from a sulphamate bath in the presence of boric acid and two additives (saccharin and FC 95™) at pH 4. Additives, such as saccharin or wetting agents, have been used for years to reduce internal stresses in the deposited material [79 and references cited therein]. In this case the deposition was carried out galvanostatically with both a titanium-rotating disc working electrode and a rotating cylinder Hull cell and was investigated by determining the polarization curves and by impedance measurements. It was found that the presence of cobalt had little effect on the deposition of nickel. Cobalt deposition was diffusion-controlled and the Co content decreased with an increase in the applied current density relative to the limiting current density. It was postulated that the simultaneous presence of saccharin and the FC95™ wetting agent hindered the sulphamate adsorption and favours Ni deposition, contrary to previous observations made with a Watts baths [79].

The electrodeposition of Co, Ni and Ni–Co alloys onto aluminium plates from a chloride bath (pH 4) to obtain magnetic thin layers was investigated by Bouyaghroumni et al. [80]. Adherent and compact deposits were obtained using direct and pulsed currents. The addition of surfactants to the bath was investigated, and a strong influence on the morphology of the deposits was observed using scanning electron microscopy and X-ray diffractometry. It was found that some cationic surfactants, that were strongly adsorbed onto aluminium at negative potentials, had a large negative effect on the deposit quality and adherence. The neutral addition agents were not adsorbed on the cathodic surface and the deposits were of a better quality than those obtained in the presence of cationic additives. Pulsed currents were helpful in improving the quality of the deposits (smooth surface and good adherence to the substrate).

3.1.3. *Electrochemical separation of nickel and cobalt*

Nickel and cobalt exhibit very similar electrochemical behaviour; therefore, this is one of the most difficult metal separations to achieve by electrodeposition. Armstrong et al. [81] reported the electroseparation of cobalt and nickel from simulated wastewater. A study of electrodeposition was performed for sulphate solutions containing either Ni(II) or Co(II) and a 1:1 mixture of both Ni(II) and Co(II), using a number of different substrate materials and configurations. The electrodeposition at stainless steel or nickel sheet electrodes was carried out under potentiostatic control. The data from deposition experiments of single cations

were used to predict the extent of separation possible from solutions containing both Ni(II) and Co(II) and these predictions were compared with experiment. Deposition from a 1:1 mixture of Ni(II) and Co(II) at the optimum potential for separation produced a 90% cobalt/10% nickel alloy. The method used for the separation is a more environmentally acceptable alternative to conventional conditions since no additions were made to the solutions.

3.2. *Electrodeposition of Ni–Cu*

In the past nickel–copper alloys were studied mainly for decorative purposes, but recently they have become of interest due to their mechanical, corrosion, electrical, and catalytic properties. Nickel–copper alloys are extensively used in industrial applications, such as ships, power stations, heat exchangers, and generally in salt-water areas. With a relatively high Ni content, the alloy is frequently used with polluted water and in pipelines or marine applications. Further applications are the use of Ni–Cu condenser tubes for saline environments as well as being employed as hydrogenation and dehydrogenation catalysts [82]. The widespread use of these alloys depends on a combination of good corrosion resistance and excellent workability as well as high thermal and electrical conductivity [83, 84].

The electrochemical preparation of these alloys has been widely studied. Citrate and pyrophosphate baths have been used most frequently and particular attention has been paid to the deposition of Ni–Cu coatings onto compact electrodes or substrates. Early work was reviewed by Roos [85] and Brenner [62].

The standard reduction potentials for copper and nickel are far apart but to obtain good alloys the potentials need to be similar. This is usually achieved for mixtures by shifting the deposition potential of the nobler component to a more negative value, either by changing the activity of the discharging ions, by adding a suitable complex-forming substance, or by inhibiting the rate of reduction of the more noble metal. The influence of additives and changes on the electrolysis parameters are also important to produce homogeneous deposits without dendritic formations.

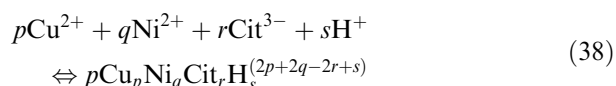
Changing the current density of the process has been shown to be another route to make the deposition potentials more similar [86]. An increase in current density caused the cathode potential to become more negative and this condition should increase the proportion of less noble metal in the deposit. At a low current density, the coating was copper-coloured and was bright, uniform, smooth, and metallic. At a higher current density it was greyish with a black powdery nature. The effect of stirring the bath has also been studied. An increase in mass transfer during stirring increased the copper content of the deposit. The coating quality also changed from a non-metallic, black powdery in the unstirred condition to a metallic, reddish brown coating under the stirred conditions.

3.2.1. Influence of electrochemical conditions

If sodium citrate is added to a sulphate electrolyte it acts as brightening, levelling and buffering agent, thus eliminating the need for other additives [86]. A slight increase in the NiSO₄ concentration in the bath has no effect on the composition of the alloy. On the other hand, a slight increase or decrease in the CuSO₄ concentration or an increase in the concentration of sodium citrate led to changes in the copper content of the deposited alloy. With the increase in pH from 8.5 to 9.5, the copper content in the deposit increased.

Schlesinger and Paunovic [87] also described an electrolyte which consisted of nickel sulphate, copper sulphate and sodium citrate. This gave a pink coating at pH 3–4 and a low current density due to the preferential deposition of copper. At higher current densities silver layers were produced in which nickel dominated.

Green et al. [88] discussed the stability of citrate electrolytes for the electrodeposition of copper–nickel alloys. The formation of metal citrate complexes was represented by the general reaction:



where p , q , r , s were stoichiometric coefficients. It was found that electrolytes operating at pH 4.12 and 4.06 were unstable due to the formation of an insoluble citrate complex dihydrate, usually formulated as Cu₂C₆H₄O₇·2H₂O [89, 90], which formed a blue precipitate after a few days. In some experiments, citrate solutions at pH 6.0 proved to be stable. The polarization data showed that the electrochemical behaviour of citrate electrolytes at different pH values differed. The polarization curves obtained in the pH 4 electrolyte corresponded to the diffusion-limited deposition of copper. However, copper deposition from a pH 6 electrolyte occurred at a more negative potential under mixed activation and diffusion control. The shift in the deposition potential of copper reflected differences in the standard potentials and exchange current densities of the dominant copper species at the two pH values. Ni–Cu alloys deposited from the various citrate electrolytes had comparable current efficiencies, compositions, and morphologies. The stability of the bath did not affect the deposit quality, when examined by scanning electron microscopy.

Ni–Cu alloy films of various compositions were obtained using glycine as the complexing agent [91]. The composition of the deposited films could be controlled by bath composition and pH, over the 4–8 range. The Ni content in the deposit was highest at pH 5 to 6, when the deposition potentials of Cu and Ni were most similar. The Cu content was lowest at pH > 5 and decreased on decreasing the concentration of Cu²⁺. Mass transport was the rate-determining step for the electrodeposition of Cu at the potentials at which codeposition of Cu and Ni occurred. The surface morphology of the film was determined using SEM

and atomic emission spectrometry. At pH 4 and 8 the surface morphologies of the films were rough, however, films deposited at pH from 5 to 6 were smooth. The reason for the surface roughness of the film was the high degree of complex formation. The crystallographic structure of all the deposited alloy films consisting of single solid solution was determined by X-ray diffractometry.

The addition of small amounts of sodium tetraborate was effective in improving the quality of the nickel–copper alloy deposited from pyrophosphate baths [92]. The result was a smooth and fine-grained, rich and lustrous nickel deposit because the tetraborate prevented a rise in the pH at the electrode/electrolyte interface above 9.5 and hence the formation of insoluble nickel hydroxides. The effects of the bath composition and operating conditions on the electrodeposition of nickel–copper alloys from a pyrophosphate–tetraborate bath onto a platinum working electrode have been studied [93]. The composition was influenced by the pyrophosphate concentration, pH of the bath, metal ion ratio, and presence of citrate ions. Pyrophosphate ions facilitated the co-deposition of nickel and copper, because it shifted the deposition potentials of each metal closer to each other. An increase in the pyrophosphate concentration suppressed the nickel deposition, but did not affect the copper deposition. Citrate ions were effective in improving the surface appearance and stability of the plating bath.

3.3. Electrodeposition of selected important ternary alloys

Ni–Co–Fe ternary alloys have also received much attention recently because of their unique magnetic and thermophysical properties [63]. For example, an electrodeposited Co₇₃Ni₁₅Fe₁₂ alloy, characterised by a high saturation magnetic flux density and resistivity, was used for the thin film magnetic heads in an ultrahigh density recording [94]. Super Invar, Fe₆₄Ni₃₁Co₅, has a low thermal expansion and is used in microwave guides, space craft optics and laser housings [95].

The anomalous electrodeposition of an interesting Ni–Co–Fe ternary alloy from a simple sulphate bath at pH 3 onto a copper rotating cylinder electrode was examined by Zhuang and Podlaha [63]. They demonstrated that Ni deposition was inhibited in the ternary system, while Fe deposition was enhanced in comparison to single-metal depositions. Both catalytic and inhibiting effects were observed for Co deposition.

Giz et al. [96] described the development of an acetate bath for the electrochemical co-deposition of Ni–Cu–Fe electrodes onto mild steel substrates at low pH. The acetate bath was stable for several weeks and produced electrodes with good performance for chlor-alkali electrolysis. The physical characterisation of the electrode surface used X-ray absorption spectroscopy, scanning electron microscopy and energy dispersive analysis.

4. Electrodeposition of multilayers

Many investigators have looked for different combinations of metals and better substrates to improve the properties of multilayer deposits. There are two different electrochemical techniques to plate multilayer thin films, dual baths and a single bath. In the dual bath technique, alternate layers of two different metals are deposited from two separate electrolyte solutions by transferring the substrate from one bath to another. In the single bath technique, the layers are obtained by depositing the noble component at the diffusion limiting current and then plating the less noble component under kinetic control. The disadvantage of this method is that some more noble metal is co-deposited during the deposition of less noble component and it is not possible to prepare a pure ferromagnetic layer. However, the impurity level of the more noble metal in the ferromagnetic layer can be kept low by using an electrolyte solution containing a 10–20 times higher concentrations of the less noble metal ion compared to the more noble metal.

Magnetic multilayers, which exhibit the giant magnetoresistance (GMR) effect, have been the subject of numerous studies because their potential for technological applications. In particular, good magnetic properties with minimum film stress are essential for magnetic materials, such as magnetoresistive sensors and magnetic recording devices. GMR is displayed by a wide variety of inhomogeneous magnetic nanostructures comprising magnetic layers separated by thin non-ferromagnetic metallic spacer layers. Magnetoresistive materials are used in many applications for detecting magnetic fields [97]. There is also great interest in the fabrication of nano-structured magnetic materials, e.g., multilayers, nano-wires, nano-tubes, nano-rods and nano-particles, to employ in nano-devices, including nano-electronics, spintronics, drug delivery and bioseparation systems. Although such nano-structured materials are generally produced by high-vacuum techniques, such as sputtering and molecular beam epitaxy, electrodeposition of multilayers is an alternative technique [98, 99]. Attention was paid to multilayers consisting of combinations of metals, such as nickel, copper and cobalt, and to the role of electrochemical parameters during their preparation. The properties of multilayer deposits were affected by the deposition potential, electrolyte composition, pH, additives, substrates and the voltage control methods.

Nickel/copper multilayers have been electrodeposited from sulphamate baths containing nickel and copper ions by alternating potential pulses [100]. Different electrochemical transient techniques were employed. In copper-free nickel sulphamate baths, the nucleation of hemispherically shaped nickel proceeded initially under electron transfer control. The growth rate of nuclei increased exponentially with the potential from 1 nm s^{-1} at -0.895 V to 50 nm s^{-1} at -1.3 V . At applied potentials more negative than -1.3 V , the film was cracked due to the simultaneous formation of

electrodeposited nickel and nickel hydroxide on the surface caused by a sharp increase in the pH. In the presence of copper ions, the electrodeposition of pure copper took place between -0.05 to -0.8 V . Copper deposition occurred under mass transfer control below -0.25 V because of the low copper ion concentrations. The co-deposition of nickel with copper occurred at potentials more negative than -0.85 V . The relative amount of copper co-deposited decreased with decreasing potential. The current transient behaviour of nickel also changed as a result of the copper co-deposition. Nano-thick Ni/Cu multilayers were electrodeposited onto platinum and onto gold sputtered silicon. The optimum potential range for nickel was between -1.20 and -1.25 V to minimize the copper content and to prevent the formation of nickel hydroxide and nickel hydride. The optimum deposition potential range for copper was between -0.4 and -0.8 V . The optimum thicknesses for the Ni and Cu layers were approximately 10 and 0.5 nm, respectively. The electrical resistivity increased on increasing the nickel thickness or decreasing the copper thickness. X-ray diffraction patterns showed good crystallinity of the Ni/Cu multilayers, SEM showed good lamellar Ni/Cu multilayers. The interface structures of the electrodeposited Ni and the Cu layers were polycrystalline with a dominant fibre texture [101].

Multilayered Ni/Cu deposits have been produced on rotating cylinder electrodes from a citrate electrolyte [102]. The modulation was 20 and 10 nm for the nickel and copper sub-layers, respectively. Multilayer deposits of the same modulation were prepared by using two different current densities for the deposition of the copper sub-layer, corresponding to kinetic control or to mixed mass transport and kinetic control of the electrode reaction. Depending on the applied current density for the copper deposition, a columnar structure of large grains or an equiaxed structure comprised of small non-oriented grains were obtained. The results showed that by modifying the deposition conditions for copper, it is possible to alter the grain size of the multilayered alloy without changing the modulation.

A detailed account of the preparation of direct current plated Ni–Cu alloys and two-pulse plated $\text{Ni}_{81}\text{Cu}_{19}/\text{Cu}$ multilayers from a sulphate–citrate electrolyte have been reported [103]. The electrodeposited coatings were produced on polycrystalline Ti and Cu substrates. Three different kinds of coatings were prepared by galvanostatic electrodeposition using various deposition current forms. A homogenous Ni–Cu alloy was obtained using a single long deposition pulse. Deposits plated with direct current at a lower current density contained only Cu metal. In deposits consisting of a Ni–Cu alloy, the Ni content increased rapidly with increasing current density. A second type of Ni–Cu alloy was produced by conventional pulse plating with the application of short deposition current pulses separated by a fixed period of zero current. Nano-scale multilayered $\text{Ni}_{81}\text{Cu}_{19}/\text{Cu}$ deposits were formed by two-pulse plating using alter-

nating cathodic current pulses. Magnetometric measurements indicated the presence of a GMR contribution as a function of the magnetic and non-magnetic layers. The formation of a chemically intermixed interface between the layers was inherent to the electrodeposition preparation technique that was used.

Thin Cu/Ni multilayers were also deposited on a rotating disk electrode by square-wave potentiostatic pulses or galvanostatic pulses. Alternate layers of Ni of nominal thickness from a few angstroms to a few microns separated by a copper film have been electrodeposited from Watts nickel baths containing 50 to 1000 ppm Cu^{2+} ions [104–106]. Factors affecting the deposition, included the mass transfer rate, the copper ion concentration, temperature, and applied current density. The thickness and deposition rate were monitored *in situ* with a quartz microbalance to explain the physical properties of the materials. The growth mechanism and structure of the Cu/Ni multilayers was studied both electrochemically and through transmission electron microscopy [107].

Yahalom and Zadok [108] investigated the production of alloys possessing a high elastic modulus and high magnetic properties. Using a pulse technique the electrodeposition of at least two metals was obtained, characterized by a redox potential gap of at least 0.1 V between metals. The layers of the metals were substantially pure and formed an integral and coherent structure with unique properties, such as high modulus of elasticity, high magnetic susceptibility, and excellent corrosion resistance especially against pitting and other types of localized attack.

The method was demonstrated for the production of binary composition-modulated alloys by the electrodeposition of a nickel–copper couple [109]. Salts of the two component metals were dissolved in a common Watts electrolyte. Traces of ions of metal A were introduced into a concentrate solution of metal B (A is nobler than B). At a low polarization potential, the rate of reduction of metal A was slow and controlled by diffusion, while metal B was deposited rapidly at a rate determined by its activation polarization constants. The potential was pulsed alternately between values above and below the reduction potential of the less noble component to form a modulated structure composed alternately of pure layers. The composition-modulated alloys were analysed by Auger spectroscopy and X-ray diffractometry. The results showed that the nickel layer contained small amounts of copper.

Evidence was reported of a large composition modulation in electrodeposited Cu/Ni films on a stainless steel substrate from a nickel sulphate solution, containing Cu^{2+} as sulphate [110]. The evidence of the formation of thin-films was obtained by electron energy loss microscopy and by high-resolution transmission electron microscopy. The resulting TEM image showed a layered structure with light coloured Cu layers separated by dark coloured Ni layers, each approximately 10 nm thick. Compositionally modulated alloys exhibit unique prop-

erties compared with the pure metals or their homogeneous alloys. The lattice parameters, mechanical and magnetic properties of these alloys are dependent on the thickness of the layers in the composite.

Ni/Cu multilayers electrodeposited by the dual bath technique onto copper substrates at room temperature were studied by Lassri and co-workers [111]. The Cu layers formed incomplete films, which lead to a partial contact between successive Ni layers. Different concentration of electrolytes caused different thicknesses of the layers. The magnetic properties were studied by magnetic measurements and ferromagnetic resonance.

If the layer thickness in a metallic Ni and Cu multilayer is reduced, at some point the layers will become discontinuous and there will be a transition to a mono-layered heterogeneous alloy. Kazeminezhad and Schwarzacher [112] studied the transition from electrodeposited multilayers to an alloy for the Ni–Cu system. The substrates were Au films evaporated onto glass or polycrystalline Cu plates. The magnetic moment of the Ni atoms in very thin Ni films was constant, suggesting a preferred Ni cluster size in these alloy films.

Ni–Cu/Cu multilayers have been grown [113], under potentiostatic conditions on polycrystalline Cu substrates from electrolytes with different pH values. The deposition potentials were chosen to yield a deposit with a metallic appearance, therefore -0.2 V and -1.7 V were selected for the Cu and Ni deposition, respectively. The transient curves for the Cu deposition had the same shape at each pH value, while for the Ni deposition the curves appeared to have different shapes. This indicated that the Ni layers had different growth modes at different pHs. The multilayers grown at a higher electrolyte pH (3.0) had rougher surfaces compared to those obtained at a lower pH (2.0). The results of chemical analysis, structural and magnetotransport characteristics as well as the observed variation of GMR with the pH of the electrolyte were discussed. The films exhibited larger GMR values when they were grown from a lower pH electrolyte. It has been shown that structural and compositional effects can contribute to the observed changes in the GMR magnitude with pH.

Nabiyouni and Schwarzacher [114] presented a comprehensive study of the structural and magnetoresistive properties of electrodeposited Ni/Cu and Ni–Co/Cu multilayers on a polycrystalline Cu substrates. The samples were grown under potentiostatic control. The deposition potentials were -1.6 V for the Ni or Ni–Co layer and -0.2 V for the Cu layer. The multilayers were characterized using high angle X-ray diffractometry, which indicate that all the samples exactly followed their substrate textures and crystal orientations. Cross-section transmission electron microscopy showed that both the microstructure and the preferred orientation were influenced by the preparation conditions. The GMR values for the Ni–Co/Cu multilayers were significantly higher than for the Ni/Cu multilayers. These results could be attributed to the

magnetization in Co being about three times larger than in Ni.

Ni–Co (Cu)/Cu multilayers consisting of 50 and 200 bi-layers were deposited from a citrate electrolyte onto a Ti–Au coated quartz disc in a flow channel cell by a dual pulse plating method [115]. The dissolution of the less noble ferromagnetic components during pulse plating was studied using an oscilloscope and cyclic voltammetry. The dissolution was suppressed due to the passivation of the ferromagnetic layer preceding the deposition of a further atomic layer of the non-magnetic component. The presence of nickel in the electrolyte as well as in the sandwich deposit insured the passivation of the ferromagnetic layer, which prevented the dissolution of the cobalt. Atomic force microscopy showed that the roughness of the ferromagnetic surface increased with an increase in layer thickness from 6 to 10 nm, whereas the roughness of the non-magnetic surface did not change significantly. Magnetoresistance measurements showed that the multilayers of this type exhibit GMR.

The electrodeposition of thin films and multilayers of the metals Cu, Co and Ni directly on the surface of n-type silicon substrates were studied by Pasa and Schwarzacher [116]. Different aqueous electrolytes containing sulphates or sulphamates of the metals and supporting additives were used. The deposits were prepared under potentiostatic conditions. Aspects related to the deposition process as well as the deposited layers were investigated by cyclic voltammetry, current transients, scanning electron microscopy, Rutherford backscattering, and magnetoresistance measurements. Ni–Co–Cu/Cu magnetic multilayers were prepared by application of the potential between -0.3 V for the non-magnetic layer (Cu) and -2.3 V for the ferromagnetic one (Ni–Co–Cu). The electric current that passed through the cell determined the thicknesses of the individual layers. The micrographs showed the layers had a compact metallic appearance and a granular morphology. Depending on the additives used, different nucleation and growth mechanisms were observed.

5. Electrodeposition on powder substrates

Electrochemical techniques are frequently used industrially for the production of metallic coatings of various compositions and properties with the aims of improving service life, to widen the application of many materials, as well as the preparation of novel materials with unusual properties. For example, the uniform thicknesses of the coatings resulting from electrochemical preparation processes, enables high-quality modified powder materials to be obtained for powder metallurgy. By using a fluidised bed an even, uniform and stable metallic coating can be deposited onto powder substrates [117–120].

The electrochemical plating of powders was studied experimentally as well as theoretically for the deposition of one-component Ni and Cu coatings and binary Ni-based (Ni–Cu, Ni–Co) coatings onto a Fe powder and onto hollow Fe powder particles in an electrolytic cell with a fluidised bed cathode [121–123]. The mechanism of these processes was investigated in detail.

In order to determine the surface area of the powder taking part in the electrode reaction, a so-called working volume model was suggested and verified [124, 125]. The influence of the concentration of the powder in the electrolyte, intensity of stirring, particle size fraction, and current intensity, on the efficiency of the electrodeposition onto powder particles was established [124, 126–128]. The effect of inhibition of the reaction due to an increase of the pH of electrolyte as a result of simultaneous hydrogen evolution was explained [122]. A probable mechanism of charge transfer through the heterogeneous system in the fluidised bed was suggested. The role of the solid powder particles in the transfer of charge and a dependence on suspension density and rate of stirring was elucidated [129–133].

The electrodeposition of metallic Cu and Ni and binary Ni–Cu coatings onto Fe hollow spheres was investigated by Šupicová et al. [134]. They compared a non-electrochemically derived coating copper coating with an electrodeposited copper layer. The coatings prepared by electroplating were much stronger, harder and more uniformly distributed.

The electrolytic deposition of two-component Ni–Cu coatings onto Fe powder particles in a fluidised bed was studied [135, 136]. The influence of the ratio of Ni(II) to Cu(II) salts in the electrolyte, of the addition of sodium citrate as a complexing agent to the electrolyte, and of the current density with respect to the total surface of compact and dispersed electrodes were investigated. The process was influenced by the spontaneous current-free deposition of Cu, which was suppressed by the addition of sodium citrate to the electrolyte as a complexing agent. The electrolytic deposition of Ni was highly preferred on a stainless steel compact cathode as well as on powder adhered to it. The deposition of the less noble Ni was facilitated mainly by its large excess in the electrolyte and by an increase in current density. A large portion of the charge was consumed by the process on a compact electrode and by hydrogen evolution. However, under optimum conditions the quality as well as the homogeneity of the coating on the powder was sufficiently high to compensate for these losses and to substantiate the application of such process. The conditions were reported for depositing a two-component Ni–Cu coating of a required composition, appearance, quality, and adherence onto Fe powder particles [135].

The influences of the hydrodynamic parameters of the fluidised bed, such as particle size, concentration of particles in the plating bath, and the rotation speed of the bed, on the deposition process were studied [136]. With increasing particle size and decreasing suspension density, the surface area decreased and, consequently,

the total amount of deposit was reduced. Another important factor was the contact of the powder particles with the current carrying compact electrode, during which the deposition of Ni is possible. This influence was seen in a decrease in the Ni-Cu ratio in the deposit with increased particle size and rotation speed.

6. Conclusions

Electrochemical processes play a very important role in the preparation of a range of materials. Nickel, cobalt, iron, and their alloys are important engineering materials in many applications because of their unique properties. Interest in understanding the deposition of these functional materials from aqueous media has expanded in recent years. The electrochemistry of the deposition process has been analysed by cyclic or stripping voltammetry, electrochemical quartz crystal microbalances, current transients, impedance, ellipsometric and amperometric investigations, and modelling techniques. Deposits were analysed by scanning electron microscopy, metallographic or transmission electron microscopy, and X-ray diffractometry.

In comparison to other methods the electrochemical deposition of coatings has advantages as it can take place at room temperature and pressure, uses relatively cheap and economically modest equipment, and the process can be easily controlled.

Acknowledgements

Financial support from the Slovak Grant Agency VEGA under project No.1/2118/05 is gratefully acknowledged.

References

- D. Landolt, *J. Electroanal. Chem.* **149** (2002) S9.
- G.A. DiBari, *Metal Finish.* **84** (1986) 23.
- D.J. Evans, *Trans. Faraday Soc.* **54** (1958) 1086.
- J. Matulis and R. Slizys, *Electrochim. Acta* **9** (1964) 1177.
- E. Heusler and L. Gaiser, *Electrochim. Acta* **13** (1968) 59.
- R. Weil and H.C. Cook, *J. Electrochem. Soc.* **109** (1962) 295.
- R. Weil, W.N. Jacobus and S.J. DeMay, *J. Electrochem. Soc.* **111** (1964) 1046.
- J.A.G. Ives, J.W. Edington and G.P. Rothwell, *Electrochim. Acta* **15** (1970) 1797.
- J.O.M. Bockris, D. Drazic and A.R. Despic, *Electrochim. Acta* **4** (1961) 325.
- C.S. Lin, P.C. Hsu, L. Chang and C.H. Chen, *J. Appl. Electrochem.* **31** (2001) 925.
- A. Saraby-Reintjes and M. Fleischmann, *Electrochim. Acta* **29** (1984) 557.
- P. Allongue, L. Cagnon, C. Gomes, A. Gündel and V. Costa, *Surf. Sci.* **557** (2004) 41.
- K.Y. Sasaki and J.B. Talbot, *J. Electrochem. Soc.* **147** (2000) 189.
- S. Hessami and C.W. Tobias, *J. Electrochem. Soc.* **136** (1989) 3611.
- M. Matlosz, *J. Electrochem. Soc.* **140** (1993) 2272.
- C.Q. Cui and J.Y. Lee, *Electrochim. Acta* **40** (1995) 1653.
- R. Oriňáková, L. Trnková, M. Gálová and M. Šupicová, *Electrochim. Acta* **49** (2004) 3587.
- M. Šupicová, R. Rozik, L. Trnková, R. Oriňáková and M. Gálová, *J. Solid State Electrochem.* **10** (2006) 61.
- J. Ji and W.C.H. Cooper, *Electrochim. Acta* **41** (1996) 1549.
- E. Gómez, C. Müller, W.G. Proud and E. Vallés, *J. Appl. Electrochem.* **22** (1992) 872.
- I. Epelboin and R. Wiart, *J. Electrochem. Soc.* **118** (1971) 1577.
- I. Epelboin, M. Jousselein and R. Wiart, *J. Electroanal. Chem.* **101** (1979) 281.
- I. Epelboin, M. Jousselein and R. Wiart, *J. Electroanal. Chem.* **119** (1981) 61.
- M. Froment and R. Wiart, *Electrochim. Acta* **8** (1963) 481.
- E. Chassaing, M. Jousselein and R. Wiart, *J. Electroanal. Chem.* **157** (1983) 75.
- R. Wiart, *Electrochim. Acta* **35** (1990) 1587.
- W.G. Proud and C. Müller, *Electrochim. Acta* **38** (1993) 405.
- M. Holm and T.J. O'Keefe, *J. Appl. Electrochem.* **30** (2000) 1125.
- M. Fleischmann and A. Saraby-Reintjes, *Electrochim. Acta* **29** (1984) 69.
- Chr. Bozhkov, Chr. Tzvetkova, St. Rashkov, A. Budniok and A. Budniok, *J. Electroanal. Chem.* **296** (1990) 453.
- M.Y. Abyaneh, *J. Electroanal. Chem.* **530** (2002) 82.
- M.Y. Abyaneh and M. Fleischmann, *J. Electroanal. Chem.* **530** (2002) 89.
- M.Y. Abyaneh, *J. Electroanal. Chem.* **530** (2002) 96.
- M.Y. Abyaneh, W. Visscher and E. Barendrecht, *Electrochim. Acta* **28** (1983) 285.
- E. Trevisan-Souteyrand, G. Maurin and D. Mercier, *J. Electroanal. Chem.* **161** (1984) 17.
- J.A.D. Jensen, P. Pocwiadowski, P.O.A. Persson, L. Hultman and P. Moller, *Chem. Phys. Lett.* **368** (2003) 732.
- G. Lemaire, P. Héban and G.S. Picard, *J. Mol. Struct.* **419** (1997) 1.
- M. Saitou, T. Chinen and Y. Odo, *Surf. Coat. Technol.* **115** (1999) 282.
- F. Lantelme, A. Seghioeur and A. Derja, *J. Appl. Electrochem.* **28** (1998) 907.
- P. Evans, C. Scheck, R. Schad and G. Zangari, *J. Magn. Mater.* **260** (2003) 467.
- J. Amblard, M. Froment, G. Maurin, N. Spyrellis and E. Trevisan-Souteyrand, *Electrochim. Acta* **28** (1983) 909.
- J. Amblard, M. Froment, G. Maurin, D. Mercier and E. Trevisan-Pikacz, *J. Electroanal. Chem.* **134** (1982) 345.
- J. Amblard, M. Froment and N. Spyrellis, *Surf. Technol.* **5** (1977) 205.
- D. Mockute and G. Bernotiene, *Surf. Coat. Technol.* **135** (2000) 42.
- D. Mockute, G. Bernotiene and R. Vilkaite, *Surf. Coat. Technol.* **160** (2002) 152.
- U.S. Mohanty, B.C. Tripathy, P. Singh and S.C. Das, *J. Electroanal. Chem.* **526** (2002) 63.
- U.S. Mohanty, B.C. Tripathy, P. Singh and S.C. Das, *J. Appl. Electrochem.* **31** (2001) 579.
- U.S. Mohanty, B.C. Tripathy, P. Singh and S.C. Das, *J. Appl. Electrochem.* **31** (2001) 969.
- H. Ferkel, B. Müller and W. Riehemann, *Mat. Sci. Eng. A* **234-236** (1997) 474.
- K.M. Ibrahim, A.A. Aal and Z.A. Hamid, *Int. J. Cast Met. Res.* **18** (2005) 315.
- A. Serek and A. Budniok, *Curr. Appl. Phys.* **2** (2002) 193.
- E. Gómez, R. Pollina and E. Vallés, *J. Electroanal. Chem.* **386** (1995) 45.
- E. Vallés, R. Pollina and E. Gómez, *J. Appl. Electrochem.* **23** (1993) 508.
- E. Gómez, C. Müller, R. Pollina, M. Sarret and E. Vallés, *J. Electroanal. Chem.* **333** (1992) 47.
- A.N. Correia, S.A.S. Machado and L.A. Avaca, *J. Electroanal. Chem.* **488** (2000) 110.
- A.N. Correia and S.A.S. Machado, *Electrochim. Acta* **45** (2000) 1733.
- A.N. Correia and S.A.S. Machado, *Electrochim. Acta* **43** (1998) 367.

58. K.D. Song, K.B. Kim, S.H. Han and H.K. Lee, *Electrochem. Commun.* **5** (2003) 460.
59. J.O'M Bockris and E.C. Potter, *J. Chem. Phys.* **20** (1952) 614.
60. H. Liebscher, *Z. Phys. Chem.* **208** (1999) 183.
61. E. Gómez, J. Ramirez and E. Vallés, *J. Appl. Electrochem.* **28** (1998) 71.
62. A. Brenner, *Electrodeposition of Alloys I* (Academic Press, New York, 1963).
63. Y. Zhuang and E.J. Podlaha, *J. Electrochem. Soc.* **147** (2000) 2231.
64. N. Zech, E.J. Podlaha and D. Landolt, *J. Electrochem. Soc.* **146** (1999) 2892.
65. H. Dahms and I.M. Croll, *J. Electrochem. Soc.* **112** (1965) 771.
66. S. Hessami and C.W. Tobias, *J. Electrochem. Soc.* **136** (1989) 4611.
67. W.C. Grande and J.B. Talbot, *J. Electrochem. Soc.* **140** (1993) 675.
68. Ch-Ch. Hu and A. Bai, *J. Electrochem. Soc.* **149** (2002) C615.
69. D. Golodnitsky, N.V. Gudin and G.A. Volynuk, *J. Electrochem. Soc.* **147** (2000) 4156.
70. Ch. Fan and D.L. Piron, *Electrochim. Acta* **41** (1996) 1713.
71. A. Bai and Ch-Ch. Hu, *Electrochim. Acta* **47** (2002) 3447.
72. N. Zech, E.J. Podlaha and D. Landolt, *J. Electrochem. Soc.* **146** (1999) 2886.
73. D. Landolt, E.J. Podlaha and N. Zech, *Z. Phys. Chem.* **208** (1999) 167.
74. M.R. Barbosa, L.M. Gassa and E.R. Ruiz, *J. Solid State Electrochem.* **6** (2001) 1.
75. C. Lupi and D. Pilone, *Minerals Eng.* **14** (2001) 1403.
76. D. Golodnitsky, N.V. Gudin and G.A. Volynuk, *Plat. Surf. Finish.* **85** (1998) 65.
77. D. Golodnitsky, Y. Rosenberg and A. Ulus, *Electrochim. Acta* **47** (2002) 2707.
78. L. Burzyńska and E. Rudnik, *Hydrometallurgy* **54** (2000) 133.
79. S. Goldbach, R. de Kermadec and F. Lapique, *J. Appl. Electrochem.* **30** (2000) 277.
80. A. Bouyaghroumni, P. Versaud and O. Vittori, *Can. Metall. Q.* **35** (1996) 245.
81. R.D. Armstrong, M. Todd, J.W. Atkinson and K. Scott, *J. Appl. Electrochem.* **27** (1997) 965.
82. I. Milošev and M. Metikoš-Huković, *J. Appl. Electrochem.* **29** (1999) 393.
83. W.A. Badawy, K.M. Ismail and A.M. Fathi, *J. Appl. Electrochem.* **35** (2005) 879.
84. K.M. Ismail, A.M. Fathi and W.A. Badawy, *J. Appl. Electrochem.* **34** (2004) 823.
85. J.R. Roos, J.P. Celis, C. Buelens and D. Goris, *Proc. Metall.* **3** (1984) 177.
86. S.K. Gosh, A.K. Grower, G.K. Dey and M.K. Totlani, *Surf. Coat. Technol.* **126** (2000) 48.
87. M. Schlesinger and M. Paunovic, *Modern Electroplating* (John Wiley & Sons Inc., New York, 2000).
88. T.A. Green, A.E. Russell and S. Roy, *J. Electrochem. Soc.* **145** (1998) 875.
89. R.W. Parry and F.W. Dubois, *J. Am. Chem. Soc.* **74** (1952) 3749.
90. D. Mastropaolo, D.A. Powers, J.A. Potenza and H.J. Schugar, *Inorg. Chem.* **15** (1976) 1444.
91. I. Mizushima, M. Chikazawa and T. Watanabe, *J. Electrochem. Soc.* **143** (1996) 1978.
92. M. Ishikawa, H. Enomoto, M. Matsuoka and C. Iwakura, *Electrochim. Acta* **39** (1994) 2153.
93. M. Ishikawa, H. Enomoto, M. Matsuoka and C. Iwakura, *Electrochim. Acta* **40** (1995) 1663.
94. T. Osaka, *Electrochim. Acta* **42** (1997) 3015.
95. M. Takai, K. Hayashi, M. Aoyagi and T. Osaka, *J. Electrochem. Soc.* **144** (1997) L203.
96. M.J. Giz, M.C. Mrengo, E.A. Ticianelli and E.R. Gonzalez, *Ecl. Quim., Sao Paulo* **28** (2003) 21.
97. S.S.P. Parkin, *IBM J. Res. Develop.* **42** (1998) 3.
98. C.A. Ross, *Ann. Rev. Mater. Sci.* **24** (1994) 159.
99. W. Schwarzacher and D.S. Lashmore, *IEEE Trans. Magn.* **32** (1996) 3133.
100. N.V. Myung and K. Nobe, *Plat. Surf. Finish.* **87**(6) (2000) 125.
101. H. El Fanity, M. Bouanani, H. Lassri, F. Cherkaoui, H. Ouahmane, A. Dinia and A. Berrada, *Ann. Chim. Sci. Mater.* **24**(7) (1999) 505.
102. Ch. Bonhôte and D. Landolt, *Electrochim. Acta* **42**(15) (1997) 2407.
103. E. Tóth-Kádár, L. Péter, T. Becsei, J. Tóth, L. Pogány, T. Tarnóczy, P. Kamasa, I. Bakonyi, G. Láng, A. Cziráki and W. Schwarzacher, *J. Electrochem. Soc.* **147** (2000) 3311.
104. C.C. Yang and H.Y. Cheh, *J. Electrochem. Soc.* **142** (1995) 3034.
105. C.C. Yang and H.Y. Cheh, *J. Electrochem. Soc.* **142** (1995) 3040.
106. N. Lebbad, J. Voiron, B. Nguyen and E. Chainet, *Ann. Chim. Sci. Mater.* **20** (1995) 391.
107. L. Wang, P. Fricoteaux, K. Yuzhang, M. Troyon, P. Bonhomme, J. Douglade and A. Metrot, *Thin Solid Films* **261** (1995) 160.
108. J. Yahalom and O. Zadok, *US Patent* **4**(652) (1987) 348.
109. J. Yahalom and O. Zadok, *J. Mater. Sci.* **22** (1987) 499.
110. J. Yahalom, D.F. Tessier, R.S. Timist, A.M. Rosenfeld, D.F. Mitchell and P.T. Robinson, *J. Mater. Res.* **4** (1989) 755.
111. H. Lassri, H. Ouahmane, H. El Fanity, M. Bouanani, F. Cherkaoui and A. Berrada, *Thin Solid Films* **389** (2001) 245.
112. I. Kazeminezhad and W. Schwarzacher, *J. Magn. Magn. Mater.* **240** (2002) 467.
113. M. Alper, M.C. Baykul, L. Péter, J. Tóth and I. Bakonyi, *J. Appl. Electrochem.* **34** (2004) 841.
114. G. Nabyouni and W. Schwarzacher, *J. Crystal Growth* **275** (2005) 1259.
115. S.M.S.I. Dulal, E.A. Charles and S. Roy, *Electrochim. Acta* **49** (2004) 2041.
116. A. Pasa and W. Schwarzacher, *Phys. Stat. Sol. (a)* **173** (1999) 73.
117. R. Oriňáková, M. Kupková, E. Dudrová, M. Kabátová and M. Šupicová, *Chem. Pap.* **58** (2004) 236.
118. R. Oriňáková, M. Šupicová, H.F. Arlinghaus, M. Kupková, G. Vering and A. Oriňák, *Surf. Interf. Analysis* **36** (2004) 784.
119. D.S. Coleman and J.N. Foba, *Powder Metall.* **32** (1989) 35.
120. E. Dudrová, *Acta Metall. Slovaca* **3** (1997) 25.
121. L. Lux, M. Gálová, R. Oriňáková and A. Turoňová, *Particle Sci. Technol.* **16** (1998) 135.
122. R. Oriňáková, *Surf. Coat. Technol.* **162** (2003) 54.
123. M. Gálová, R. Oriňáková, T. Grygar, L. Lux and M. Heželová, *Particle Sci. Technol.* **19** (2001) 85.
124. L. Lux, R. Stašková and M. Gálová, *Acta Chim. – Models in Chemistry* **133** (1996) 115.
125. M. Gálová, R. Oriňáková and L. Lux, *J. Solid State Electrochem.* **2** (1998) 2.
126. A. Turoňová, M. Gálová, L. Lux and M. Gál, *J. Solid State Electrochem.* **5** (2001) 502.
127. L. Lux, R. Oriňáková and M. Gálová, *Acta Metall. Slovaca* **3** (1997) 603.
128. L. Lux, M. Gálová and R. Oriňáková, *Chem. Pap.* **52** (1998) 736.
129. M. Fleischmann and J.W. Oldfield, *J. Electroanal. Chem.* **29** (1971) 231.
130. R.E. Plimley and A.R. Wright, *Chem. Eng. Sci.* **39** (1984) 395.
131. C. Gabrielli, F. Huet, A. Sarah and G. Valentin, *J. Appl. Electrochem.* **24** (1994) 481.
132. M. Gál, M. Gálová and A. Turoňová, *Collect. Czech. Chem. Commun.* **65** (2000) 1515.
133. R. Oriňáková, H.D. Wiemhöfer, J. Paulsdorf, V. Barinková, A. Bednáriková and R. M. Smith, *J. Solid State Electrochem.* **10** (2006) 458.
134. M. Šupicová, R. Oriňáková, M. Kupková and M. Kabátová, *Surf. Coat. Technol.* **195** (2005) 130.
135. A. Turoňová, M. Gálová and M. Šupicová, *J. Solid State Electrochem.* **7** (2003) 684.
136. A. Turoňová, M. Gálová, M. Šupicová and L. Lux, *J. Solid State Electrochem.* **7** (2003) 689.